



HAL
open science

Pepsin diffusion in complex food matrices

Elham Rakhshi, Françoise Nau, Manon Hiolle, Juliane Floury

► **To cite this version:**

Elham Rakhshi, Françoise Nau, Manon Hiolle, Juliane Floury. Pepsin diffusion in complex food matrices. *Journal of Food Engineering*, 2022, 324, pp.111011. 10.1016/j.jfoodeng.2022.111011 . hal-03629567

HAL Id: hal-03629567

<https://institut-agro-rennes-angers.hal.science/hal-03629567v1>

Submitted on 22 Jul 2024

HAL is a multi-disciplinary open access archive for the deposit and dissemination of scientific research documents, whether they are published or not. The documents may come from teaching and research institutions in France or abroad, or from public or private research centers.

L'archive ouverte pluridisciplinaire **HAL**, est destinée au dépôt et à la diffusion de documents scientifiques de niveau recherche, publiés ou non, émanant des établissements d'enseignement et de recherche français ou étrangers, des laboratoires publics ou privés.



Distributed under a Creative Commons Attribution - NonCommercial - NoDerivatives 4.0 International License

1 **FULL TITLE: PEPSIN DIFFUSION IN COMPLEX FOOD MATRICES**

2 Running title. **PEPSIN DIFFUSION IN COMPLEX FOOD MATRICES**

3 Elham Rakhshi, Francoise Nau, Manon Hiolle and Juliane Floury*

4 Affiliation(s):

5 *STLO, INRAE, L'Institut Agro, 35042, Rennes, France*

6 ***Corresponding author**

7 Address: **L'Institut Agro Rennes Angers**, INRAE, UMR 1253 Science et Technologie du Lait et
8 de l'Œuf, 65 rue de St Briec, 35012 Rennes Cedex, France.

9 Tel : +33 2 23 48 54 52 ; E-mail: juliane.floury@agrocampus-ouest.fr

10

11 **Abstract**

12 Pepsin diffusion in food particles during gastric digestion is one of the main factors limiting
13 proteolysis kinetics. Diffusion coefficients of pepsin are needed as input parameters for *in silico*
14 models of digestion, but no values are currently available in real foods. The challenge of this study
15 was to apply the Fluorescent Recovery After Photobleaching (FRAP) technique to determine
16 diffusion coefficients of fluorescently labelled (FITC)-pepsin in **four realistic food matrices with**
17 **complex and heterogeneous structures** (Custard, Pudding, Sponge cake and Biscuit), but an
18 identical composition on a dry matter basis. The effective diffusion coefficients determined for
19 FITC-pepsin at 37°C ranged from 48±14 to 2±1 μm²/s for Custard and Biscuit, respectively. **A**
20 **modelling approach based on the stretched exponential equation generated a very good fit of the**
21 **experimental dataset as a function of dry matter content of the matrix.**

22 **Keywords:** Digestion, Confocal microscopy; Diffusion; FRAP; Pepsin; Food structure.

23 1. Introduction

24 It is now widely recognized that various aspects (i.e. physical, enzymatic and chemical) of the
25 human food digestion process are influenced by the physical characteristics of the ingested foods
26 (Somaratne et al., 2020a; Hiolle et al., 2020; Norton et al., 2014). In the case of so-called solid
27 foods, the stomach has been shown to be the main compartment for food disintegration. The
28 breakdown of chewed solid foods into particles of smaller sizes is the consequence of both
29 mechanical contraction of the stomach and biochemical reactions (Kong & Singh, 2010). Density,
30 texture and microstructure of foods can be critical for particle fragmentation and hydrolysis of
31 macronutrients (Dekkers et al., 2016). In such solid and complex foods made of macronutrients
32 which are intrinsically associated into complex architectures at molecular to macro length scales,
33 the rate-limiting step for macronutrient hydrolysis has been clearly shown to be the accessibility
34 of the digestive fluids and enzymes to immobilized substrates (Capuano & Janssen, 2021; Marze,
35 2013). Therefore, beyond the particle surface area, which depends on food particle size, the
36 capability of the digestive fluids and enzymes to penetrate within the porous particles is also a key
37 parameter to consider in the understanding of food digestion kinetics (Le Feunteun et al, 2021).
38 An existing consensus within the scientific community claims that gastric disintegration of protein-
39 based food particles could be modified by changing their structure (Floury et al., 2018; Hiolle et
40 al., 2020; Norton et al, 2014; Somaratne et al., 2020a; Thévenot, et al., 2017). The underlying
41 assumption is that pepsin diffusion into food matrices and subsequent rate of protein pepsinolysis
42 might be strongly correlated with the food matrix structure (Somaratne et al., 2020a; Somaratne et
43 al., 2020c; Thévenot et al., 2017). However this hypothesis still remains unproved, because of the
44 lack of available techniques to visualize the disintegration of dense food structures during gastric

45 digestion by pepsin. A quantitative investigation of pepsin diffusion in such food structures may
46 therefore contribute to a deeper understanding of food breakdown and digestion kinetics.

47 Beyond this need of better understanding the digestion mechanisms of real complex foods, using
48 both *in vitro* measurements and *in vivo* studies on humans or animals, mathematical modelling
49 classically used in food engineering offer an alternative approach that can provide information that
50 is time-intensive and sometimes impossible to obtain experimentally. Sicard et al. (2018) built a
51 reaction-diffusion model for gastric meat digestion that accounts for simultaneous pepsin diffusion
52 in bolus particles, pH-dependence of pepsin activity, proton diffusion and meat buffering capacity,
53 as well as gastric fluid velocity. Mass transfers of pepsin and of protons were described by Fickian
54 diffusions inside spherical meat particles of constant diameter greater than half a millimetre as a
55 first assumption. Moreover, due to lack of available data, the value of the pepsin diffusion
56 coefficient was assumed equal to its estimated value in water thanks to the Stokes-Einstein
57 equation. Therefore, the improvement of such modelling approach requires a better
58 characterisation of major input physical parameters such as effective pepsin diffusion coefficients
59 in the real food media.

60 For a short time, quantitative characterization of food structure and digestive enzyme diffusion
61 within a given food matrix became feasible thanks to the recent advances in quantitative
62 microscopic techniques based on confocal laser scanning microscopy (CLSM). **Fluorescence**
63 **Recovery After Photobleaching (FRAP) technique has allowed to determine the diffusion**
64 **coefficients of pepsin in simple model food systems such as pure protein gels of casein or egg**
65 **white (Thévenot et al, 2017, Somaratne et al., 2020b). The hindered diffusion behaviour of pepsin**
66 **is affected by the microstructure of the network at constant protein concentration (Somaratne et al,**
67 **2020b). Moreover, the evolution of the effective diffusion coefficient of pepsin as a function of**

68 the protein volume fraction of the matrices could be remarkably well predicted by theoretical
69 diffusion models from polymer science (Thévenot et al., 2017).
70 However, no values for the diffusion coefficients of pepsin in real foods are currently available in
71 the literature. Indeed, FRAP is still an under applied method in food science (Loren et al 2015).
72 Successfully applying the FRAP technique in real food matrices is indeed a challenging task
73 because they are often multiphase materials consisting of gels, emulsions, foams, solutions, crystal
74 networks, amorphous and crystalline areas, etc. and heterogeneous at different length scales.
75 However, its ability to determine local diffusion properties in heterogeneous foods with high
76 precision makes it a versatile tool for understanding the mechanisms controlling diffusion in foods
77 (Loren et al 2015). For instance, CLSM combined with FRAP was exploited to study the diffusion
78 of a range of fluorescent-labeled dextrans as a function of their molecular weights within β -
79 lactoglobulin solutions and gels (Nicolai et al., 2012). Lorén et al. (2009) and Silva et al. (2013)
80 also used FRAP to measure the effective diffusion coefficients of fluorescent macromolecules
81 (RITC, or FITC-dextran from 4 kDa to 2 MDa, respectively) in model cheeses based on ultra- and
82 micro-filtered milk. Later, the FRAP technique was applied to real soft-cheese by Chapeau et al.
83 (2016), in order to investigate the relationships between molecular diffusion and food
84 microstructure.

85

86 The present study aims to determine how pepsin diffusion within real food products is affected by
87 the features of the matrix. In order to specifically address the issue of the food structure impact on
88 food digestion, model foods of same composition but different structures were needed. The
89 strategy was therefore to design four real complex foods, of identical composition on a dry matter
90 basis (including proteins, lipids and carbohydrates), but different dry matter content and structures

91 (liquid, gel, foam and solid types). Moreover, in order to obtain measurements as realistic as
92 possible, the four different food products have been designed so as to be representative of
93 commercial products: Custard, Pudding, Sponge cake and Biscuit. Effective diffusion coefficients
94 of fluorescently-labeled pepsin were determined using the FRAP technique in confocal
95 microscopy.

96

97 **2. Material and methods**

98 **2.1 Materials**

99 Food samples were prepared using wheat flour (Francine T45, Grands Moulins de Paris, Ivry Sur
100 Seine, France), extruded dehulled pea flour (Sativa 32/100, Sotexpro, Bermericourt, France),
101 powdered sugar (Saint-Louis Sucre, Paris, France), sunflower oil (Lesieur, Asnières-sur-Seine,
102 France), standard pasteurized egg yolk and granulated pasteurized egg white powders (Liot,
103 Pleumartin, France) and sterilized water. Fast Green, Nile Red, pepsin from porcine gastric mucosa
104 and FITC were purchased from Sigma-Aldrich (St. Louis, MO, USA). All reagents, unless
105 specified in the text, were provided by Sigma and were of analytical grade.

106

107 **2.2 Preparation of food matrices**

108 Four different food matrices with identical composition on a dry matter basis were designed and
109 characterized in a previous study. The complete description of the manufacturing process for these
110 matrices is detailed in Hiolle et al. (2020). Briefly, the manufacturing process consisted of the
111 following steps: 1) whisking (only for Sponge cake), 2) mixing, 3) cooking (180 °C-18 min for
112 Biscuit, 30 min for Sponge cake and 20 min for Pudding, 110 °C-20 min for Custard), 4) cooling
113 and 5) storage. A kitchen robot Thermomix® TM5 (Vorwerk, Wuppertal, Germany) was used for

114 preparation of Custard, whereas the other three matrices were cooked using a semi-professional
115 convection oven (De Dietrich, Niederbronn-Les-Bains, France). The dry basis protein,
116 carbohydrate, lipid and ash contents of all food samples were 17%, 52%, 30%, and 1%,
117 respectively. Custard was prepared just before experiments. The other three foods were frozen and
118 stored at -20 °C until use. Before freezing, the products were previously cooled to room
119 temperature and then vacuum-packed in polypropylene bags in order to avoid any water transfer.
120 At the day of use, the products were thawed at room temperature, before removing the packaging.
121 Water content was gravimetrically measured for each matrix after cooking according to the method
122 NF-V-04-282 AFNOR (1985).

123

124 2.3. Confocal Laser Scanning Microscopy imaging

125 CLSM observations were carried out using a ZEISS LSM 880 inverted confocal microscope (Carl
126 Zeiss AG, Oberkochen, Germany) set at the magnification 40× (EC Plan-Neofluar objective, Oil,
127 NA=1.30). Solid food matrices (Biscuit, Sponge cake and Pudding) were cut to squares of 5 to 6
128 mm sides and 1 mm height and then transferred onto glass slides. The dimensions were measured
129 using a digital caliper with accuracy of 1 µm.

130 Fast Green (1% w/v aqueous solution) and Nile Red (0.1% w/v 1,2-propanediol solution) were
131 used to respectively stain protein and fat components. At first, the two fluorescent dye solutions
132 were mixed at equal volumes. Then a small volume (6 µL) of the mixed solution was either placed
133 on solid food slices, or directly added to the Custard sample (600 µL). Then, the samples were
134 stored at 20 °C for a minimum duration of 30 min to let the dyes well diffuse into the solid matrices.
135 For Custard, a drop of the labelled sample was deposited on a glass slide. Subsequently, the
136 specimens were covered by cover slips sealed with several adhesive frames (Geneframe, ABgene

137 House, UK). Imaging was performed at excitation wavelengths of 488 nm and 633 nm in
138 sequential beam fluorescent mode, for fat and protein detection respectively. Pixel dwell scanning
139 rate was 1.5 μ s and pinhole was set to 1 airy unit. A GaasP detector and a PMT detector were
140 respectively used for detection of Red Nile (at a wavelength range of 500-585 nm) and Fast Green
141 (at a wavelength range of 635- 735 nm).

142 Micrographs had a resolution of 0.076 μ m/pixel and were recorded in the samples at a constant
143 depth of 10 to 15 μ m from the glass slide. Images shown in this study correspond to
144 superimpositions of images of the same area observed separately with the two detectors, with
145 proteins coded in green and fat in red. Aqueous phase and gas bubbles in the slices may appear as
146 black holes in the micrographs.

147

148 **2.4. Pepsin labeling and FRAP analysis**

149 For FRAP analysis, pepsin was fluorescently-labeled with FITC according to the manufacturer's
150 instructions as previously described by Thévenot et al. (2017). FITC-pepsin has a hydrodynamic
151 radius of 3.6 nm and an average molecular weight of 32.4 kDa (Thevenot et al., 2017). The pepsin
152 inactivation by the labelling reaction was checked by measuring the FITC-pepsin activity using
153 hemoglobin (Hb) as the substrate, according to the method described in Minekus et al. (2014). A
154 50 mg/mL stock solution of FITC-pepsin was prepared before FRAP experiments using deionized
155 water, and stored at -20 °C. Food matrices were prepared on individual glass slides as reported
156 before (section 2.3). Three μ L of the FITC-pepsin solution and 3 μ L of the 1% (w/v) Fast Green
157 aqueous solution were both added to the surface of the sample. To ensure fluorescent molecules
158 migration from the surface of sample toward its bottom, samples were kept at room temperature

159 (20 °C) for approximately 30 min before measurements. For each matrix, three different samples
160 were prepared separately to ensure the reproducibility of sample preparation.

161 Effective diffusion coefficients (D_{eff}) of FITC-pepsin were measured at a temperature of 37 °C
162 using the FRAP protocol described in Somaratne et al. (2020b) and Thévenot et al. (2017). Briefly,
163 experiments were performed on the Zeiss LSM880 equipped with a microscope cage incubator
164 using the 40× objective lens (oil immersion: NA = 1.30). FITC-pepsin was excited at a wavelength
165 of 488 nm using an argon laser system, and detected at a wavelength range of 495–580 nm. The
166 laser was set at 1% for imaging and 100% for bleaching step. Samples were observed at a constant
167 depth of 15 μm from the sample surface. The region of interest (ROI) was a 5 μm -radius circular
168 region whereas a rectangular region was selected as the background. The protein network was
169 preferred both as ROI and background, avoiding areas which contained lipid droplets and air
170 bubbles. These protein network areas were localized on each microscopic views before starting
171 FRAP experiments, using the Fast Green fluorescence at the 633 nm excitation wavelength. During
172 FRAP experiments, 20 pre-bleach images were first collected, and then the ROI was bleached
173 using 150 iterations, followed by a post-bleaching phase for which 480 images at 0.1 ms intervals
174 were captured until full fluorescent recovery in the ROI. **This FRAP procedure has been repeated**
175 **ten times on different locations in each food sample. This set of experiments was also conducted**
176 **three times on each type of matrix, resulting in an average effective diffusion coefficient value for**
177 **pepsin calculated from 30 replicate data per product (n=30).** Control FRAP experiments were
178 carried out in the same conditions to determine the diffusion coefficient of FITC-pepsin in water
179 using a 0.5 mg/mL FITC-pepsin solution.

180 Data were analyzed using FIJI software, according to the method described in Thévenot et al.
181 (2017). Briefly, both a pure isotropic diffusion in a homogeneous medium, and a two-dimensional

182 and Fickian diffusion process were assumed for the FRAP data modeling. Data fitting via nonlinear
183 least squares was conducted using RStudio software, allowing the estimation of the effective
184 diffusion coefficient of pepsin (D_{eff}). The reduced diffusion coefficient (D_r) was calculated as the
185 ratio of effective diffusion coefficient in matrices divided by the diffusion coefficient in water
186 (D_0).

187

188

189 2.5. Statistical analysis and modelling of diffusion data

190 The dataset of effective diffusion coefficients of FITC-pepsin determined in the four different food
191 matrices and the water control sample, was analyzed thanks to RStudio software using a one-way
192 analysis of variance (ANOVA) and a Tukey's paired comparison test, at a 95% confidence level.

193 Then the reduced diffusion coefficients were fitted using the empirical stretched exponential
194 equation, based on a scaling law and considered as a "universal" equation by Phillies (2016) as:

$$195 \quad D_r = D_{\text{eff}}/D_0 = \exp(-\alpha \cdot c^v) \quad [\text{Eq.1}]$$

196 where α and v represent the scaling parameters which should depend on the size of the diffusing
197 solute, and c represents the number concentration of obstacle (the polymer).

198 Data fitting was performed using Excel 2016 and its evolutionary solving method by minimizing
199 the sum of the squared distances between values of the model predictions [Eq. 1] and the
200 experimental reduced diffusion coefficient D_r . The variable parameter c was arbitrarily set as the
201 DM content, and the constant parameter v was set to 1, as recommended for a small diffusing
202 solutes (Phillies, 1986). Finally, the only unknown parameter was the constant α .

203

204

205 3. Results and discussion

206 3.1. Structural characteristics of the four matrices

207 Table 1 shows the main characteristics of the four different matrices in terms of processing
208 conditions, water content and structural properties. **These products have been empirically designed**
209 **so as to be as close as possible to commercial products, and with significantly different structures,**
210 **from a single composition except water content. Thus, these four products should enable us to**
211 **investigate the water content and structure effect only.** The Biscuit, which had the lowest water
212 content ($5.56 \% \pm 1.59$) and underwent a high cooking temperature ($180\text{ }^{\circ}\text{C}$) had a porous brittle
213 structure. The Sponge cake and the Pudding have been cooked at the same temperature ($180\text{ }^{\circ}\text{C}$)
214 but for longer durations (30 min and 20 min, respectively, vs 18 min for the Biscuit) because of
215 the higher height of the products. Moreover, these matrices had higher water contents, and the
216 Sponge cake process includes a whisking step. The result of this is that the Sponge cake was a dry,
217 aerated and porous gel, whereas the Pudding was a wet and dense gel. Custard was the only liquid
218 food with the highest water content; it was also submitted to the lowest heat treatment ($110\text{ }^{\circ}\text{C}$ for
219 20 min) and could be regarded as a thick liquid.

220 These four complex foods contained three different sources of proteins: egg white, wheat and pea
221 proteins. In Biscuit and Sponge cake, a gluten network was likely formed during mixing, with
222 plausible disulfide bonds between cysteine residues that were reinforced during cooking and
223 resulted in a dry solid matrix (Belton, 1999). Indeed, it is known that high temperature and low
224 water content in matrix containing wheat flour result in forming disulfide bonds resulting in a
225 compact network (Fischer, 2004; Shewry & Tatham, 1997). The brown color of Biscuit and
226 Sponge cake crust was a consequence of non-enzymatic reactions, specifically the Maillard and
227 caramelisation reactions, which are almost absent in the two other matrices. However, the

228 solidification of Pudding might be attributed to heat-gelation of egg proteins rather than to the
229 formation of a gluten network. Indeed, the Pudding was in a liquid form before cooking, unlike
230 Biscuit and Sponge cake which were doughy, and heat-gelation of yolk and egg white proteins is
231 known to occur at quite low temperatures: around 60 °C for egg white proteins (Yamashita et al.,
232 1998) and 75 °C for yolk proteins (Woodward & Cotterill, 1987). In Custard, although egg proteins
233 were surely denatured and partially aggregated due to cooking temperature (110 °C), the high
234 water content combined with the constant mixing prevented the formation of a continuous gel and
235 it stayed as a thick liquid product.

236 Typical confocal imaging of the four model foods are also illustrated in Table 1. The protein
237 network, represented in green, was much more continuous in the microstructure of Biscuit,
238 followed by those of Sponge cake and Pudding compared to the microstructure of Custard. This is
239 consistent with the varying water content of the food matrices, and indicates that water played an
240 expected and remarkable role in the microstructural organization. Likewise, egg white proteins
241 were gelled in the Sponge cake and the Pudding, forming a quite homogeneous protein network at
242 the microscopic scale. In Custard, only small and unconnected protein aggregates suspended in the
243 aqueous medium are visible, without any gel-like network. In all matrices, lipid phase which
244 consisted of sunflower oil and egg yolk lipids is observed as globular red droplets.

245

246 **3.2. Validation of the FRAP method to measure pepsin diffusion at 37 °C**

247 Control FRAP tests were performed to find out pepsin diffusion coefficients through food matrices
248 at 37 °C, which is the physiologically relevant temperature for human digestion. To validate the
249 accuracy of the FRAP protocol performed at 37 °C for the first time, the experimental diffusion
250 coefficient of pepsin measured in water was first compared to its corresponding theoretical value.

251 Indeed, assuming that pepsin molecules in water have a dynamic behaviour similar to the random
252 movement of particles in solution, the diffusion process is controlled by the size of the solute
253 molecule as described by the Stokes-Einstein equation:

$$254 \quad D_0 = \frac{k_B T}{6\pi\eta R_h} \quad [\text{Eq.2}]$$

255 where D_0 is the diffusion coefficient in water ($\text{m}^2\cdot\text{s}^{-1}$), k_B the Boltzmann constant ($1.38 \cdot 10^{-23} \text{ J}\cdot\text{mol}^{-1}\cdot\text{K}^{-1}$), T the absolute temperature (K), η the viscosity of the medium (Pa.s), and R_h the
256 hydrodynamic radius of the diffusing molecule (m). Given that water viscosity is 0.6915 mPa.s at
257 37 °C (310 K), and 1 mPa.s at 20 °C (293 K) (Braga et al., 2004), the diffusion coefficient of
258 pepsin in water should be theoretically 1.44 higher at 37 °C than at 20 °C. Somaratne et al. (2020b)
259 used the same FRAP protocol and data analysis as described in the present study. They measured
260 a diffusion coefficient for FITC-pepsin in water equal to $104.5 \pm 10.7 \mu\text{m}^2/\text{s}$ at a temperature of 20
261 °C. In the present study, we measured an experimental diffusion coefficient of pepsin in water
262 equal to $138 \pm 11 \mu\text{m}^2/\text{s}$ at 37 °C, which is 1.3 times higher than the value previously obtained at 20
263 °C. Experimental and theoretical ratios of $D_0(37 \text{ °C})/D_0(20 \text{ °C})$ were of the same order of
264 magnitude, with a difference of 8.5% only. The FRAP protocol was therefore considered to be
265 suited to measure the diffusion coefficient of pepsin at 37 °C.
266

267

268 **3.3. Effective and reduced diffusion coefficients of pepsin in the four food matrices**

269 Typical fluorescence recovery curves with FITC-labeled pepsin in the food matrices are presented
270 in Fig. 1, with selected FRAP images before, during, and after photo-bleaching as inserts. Protein
271 areas (in white) were preferentially selected as ROI for the three solid matrices, since FITC-pepsin
272 is hydrophilic and could not diffuse inside lipid droplets. Nearly complete fluorescence recovery
273 was observed for all the food matrices (normalized intensity close to 1 at the end of the post-

274 bleaching period), suggesting isotropic diffusion of fluorescent pepsin molecules. However,
275 distinct profiles were obtained for the different matrices, resulting in different effective diffusion
276 coefficients determined from the modelling of the experimental data, and summarized in Table 2.

277
278 First, it should be noted that the chemical labelling of pepsin with the fluorescent probe at a
279 reaction pH8 leads to a complete inactivation of the enzyme (data not shown), due to the
280 irreversible denaturation of the protein tertiary structure and thus of the active site (Kamatari et al.,
281 2003). In the present work, both enzyme diffusion and pepsinolysis reaction phenomena are
282 therefore totally decoupled. The FRAP technique allowed the quantification of the Brownian
283 motion of FITC-pepsin in the ROI, whereas classical confocal observations of the products
284 allowed the characterization of the so-called "native" matrices at the micro-scale (Table 1), and
285 the values of FITC-pepsin diffusion coefficient reported in Table 2 actually represent the diffusion
286 behaviour of the inactivated enzyme within these four different "native" matrices.

287 Second, it is noteworthy that despite both the precautions during FRAP experiments to positioned
288 as much as possible the ROI in sample areas rich in proteins, which were localized using a specific
289 fluorescent labeling (Fast-Green), and a large number of replicate data ($n = 30$), the kinetics of
290 fluorescence recovery during FRAP experiments were quite variable. The resulting standard
291 deviations (SD) values obtained for D_{eff} of FITC-pepsin in the four food products were much
292 higher, ranging between 30%-40% and up to 60% for the Pudding, compared to previous studies
293 in which the same FRAP protocol was applied to quantify FITC-pepsin diffusion coefficient in
294 pure protein matrices such as casein and egg white gels (Somaratne al., 2020b; Thévenot et al.,
295 2017). In such homogeneous and isotropic protein networks, SD values for average pepsin
296 effective diffusion coefficients were around 10 to 15% maximum. A larger variability in the mean

297 values of effective diffusion coefficients of FITC-Dextran of different sizes obtained using the
298 FRAP technique had also been obtained in real cheese matrices (Chapeau et al., 2016) compared
299 to the diffusion values of the same solutes in casein gels (Silva et al., 2013). As reported in Lorén
300 et al. (2015), structural heterogeneity of the sample greatly influences FRAP data. Therefore, the
301 high variability of the diffusion coefficient values of FITC-pepsin probably results from the high
302 local heterogeneity of the food matrices, related to their complex composition (multi-constituents)
303 and structure (multiphasic) as shown in Table 1.

304 Despite this quite high variability of FRAP data, Table 2 allows to highlight a significant increase
305 in the effective diffusion coefficient of FITC-pepsin coupled with the increasing water content of
306 the food matrices, regardless of the processing conditions and the food structures resulting
307 therefrom (Table 1). In particular, it is notable that no statistical significant difference ($p > 0.05$)
308 was observed between FITC-pepsin D_{eff} in Pudding, which can be described as a dense and
309 continuous protein gel, and Sponge cake that is an expanded and alveolar product. Since both
310 products have quite similar dry matter content (less than 10% difference), but different structures,
311 this result reinforces the dry matter content as a key parameter for the FITC-pepsin diffusion.

312

313 The corresponding reduced diffusion coefficients of FITC-pepsin was calculated in the different
314 matrices (Table2). These values allow to bring out a 10-time reduction of pepsin diffusion in
315 Pudding and Sponge cake as compared to water, while for Biscuit it is almost a 100-time reduction.
316 This suggests that protein hydrolysis by pepsin might be further much hindered by slow mass
317 transfer in Biscuit as compared to the other more humid food matrices. In Custard, the reduced
318 pepsin diffusion coefficient is only one third of the value measured in water, suggesting a

319 facilitated access of the gastric enzyme to the protein substrates in this liquid version of the food
320 matrices as compared to the solid ones.

321

322 **3.4. Toward a predicting model of pepsin diffusion in real foods?**

323 Diffusion in polymer systems like foods is a complicated process, because it depends on numerous
324 parameters, such as the diffusing solute properties, the polymer network microstructure, and the
325 solvent (Masaro & Zhu, 1999; Silva et al., 2013). Many physical models approaches describing
326 the diffusion of rigid and spherical nanoparticles in hydrogels as a function of structural
327 parameters, such as nanoparticle radius, polymer volume fraction and polymer strand radius have
328 been developed and reviewed in the literature (Amsden, 1998; de Kort et al., 2015; Masaro & Zhu,
329 1999). Those models are based on three main physical concepts, such as the obstruction effects,
330 the hydrodynamic interactions and the free volume theory.

331 In the literature more specifically dedicated to food digestion, more and more recent studies
332 highlighted that the physical properties of foods, especially their composition and microstructural
333 characteristics, are also key parameters for the mass transfer behaviour of digestive fluids and
334 enzymes within the food matrix (Grundy et al., 2016, Luo et al., 2017; Thevenot et al., 2017;
335 Somaratne et al., 2020a; Somaratne et al., 2020b). Thévenot et al. (2017) and Luo et al. (2019)
336 quantified the impact of an increasing protein concentration on the diffusion coefficients of FITC-
337 pepsin in casein gels using the FRAP, and on the diffusion coefficient of enhanced green
338 fluorescent protein (eGFP) in whey protein gels using the FCS technique, respectively. In both
339 studies, their experimental data were the most successfully fitted using the Amsden's obstruction-
340 scaling model (Amsden, 1998) and the Cukier's hydrodynamic theory (Cukier, 1984). In the
341 obstruction theory, the polymer chain network obstructs specific sites that were otherwise available

342 for the solute, and therefore reduces the available paths for diffusion (Amsden, 1998). The chains
343 themselves are considered immobile and impenetrable for the solute. In the hydrodynamic theory,
344 the friction of the solute with the medium is considered as the main cause of reduced diffusion rate
345 compared to diffusion of the solute in water (Cukier, 1984). These models would therefore allow
346 the reliable prediction of pepsin diffusion coefficients, provided the knowledge of several physical
347 parameters such as the hydrodynamic radius of pepsin solute, the polymer volume fraction and the
348 average particle size of the gel network.

349 In the present study, the large difference between the effective diffusion coefficients of pepsin in
350 Custard and the other three matrices can be mainly attributed to the difference in their water
351 content, but probably also to their different physical states : liquid versus gelled and foamed, to
352 solid products. However, due to both the high complexity and heterogeneity of the different
353 products, the parameters describing the polymer network properties requested in either Amsden or
354 Cukier's models of diffusion are unknown.

355 Based on numerous experimental diffusion data available from the literature, Phillies (1986)
356 proposed a more phenomenological approach based on the stretched exponential equation (Eq. 1)
357 to describe the diffusion behaviour of solutes like polymer and protein in hydrogels over a wide
358 range of concentrations. This flexible equation has been also largely employed to describe other
359 physical transport phenomena such as sedimentation, electrophoretic mobility and viscosity, and
360 can therefore be considered as a "universal" equation (Phillies, 2016). Figure 2 shows that, except
361 for the Biscuit, this modelling approach generated a very good fit of our experimental diffusion
362 data by simply replacing the variable parameter c , which theoretically represents the number
363 concentration of obstacle in the polymer network, by the value of the DM content of the matrix
364 (%). The constant parameter ν was set to 1, considering the pepsin as a small diffusing solute. The

365 only unknown parameter was therefore the constant α , which depends on the size of the diffusing
366 solute: the molecular weight for macromolecules or hydrodynamic radius (R_h) for smaller
367 molecules (Phillies, 1986).

368 As shown in Figure 2, the best curve fit was obtained with a value of this scaling parameter α
369 equal to 3.5. Quite strikingly, it is noteworthy that this value is here almost equal to the
370 hydrodynamic radius of FITC-pepsin, as previously measured by Thévenot et al (2017) ($R_h = 3.6$
371 nm). It means that this model approach based on the “universal” stretched exponential equation
372 would therefore allow the very reliable prediction of pepsin diffusion coefficients in real food
373 media, by simply knowing the most basic composition data such as the Dry Mater content. As
374 mentioned before, the ROI chosen for the FRAP experiments were as much as possible positioned
375 in sample areas containing mostly proteins. Consequently, our results can probably also be
376 interpreted as an estimation of the protein network density in the different food matrices, which is
377 in agreement with Thévenot et al. (2017) who reported that pepsin diffusion is hindered by
378 increasing casein concentration in dairy gels as a consequence of aggregation of proteins.

379 As observed on the plot of the natural logarithm of reduced diffusion data (Fig 2), the linearized
380 form of the equation allows highlighting that the model is not able to accurately predict the
381 effective diffusion coefficient of FITC-pepsin in the Biscuit because a much lower experimental
382 mobility ($D_r = 0.013$) is obtained, as compared to the predicted value by the model ($D_r = 0.035$).
383 In this product, the very low water content allowed to assume that the physical state of the polymer
384 network made of starch and protein had probably turned from a “rubbery” state to a “glassy” state
385 (Chevallier et al., 2000). This glass transition is known to affect both molecular mobility and
386 kinetic energy in the product (BeMiller, 2018).

387

388 **3.5. Is the hindered diffusion of pepsin really responsible for different food digestion**
389 **kinetics?**

390 Protein denaturation extent (Jin et al., 2016), and food processing practices (Morell et al., 2017)
391 can significantly influence the rates of food (proteins) digestion and absorption kinetics. In this
392 context, tailoring the food structure might enable to take control over the rate/extent of protein
393 digestion (Barbé et al., 2013; Nyemb et al., 2016; Rinaldi et al., 2014). Studying *in vitro* digestion
394 of four different types of egg white gels (EWG), Nyemb et al. (2016) attributed the observed
395 discrepancy between gel digestibilities to differences in pepsin activity stemmed from the different
396 steric hindrance within the protein gels. The dissimilar pepsin activity was hypothesized to be a
397 consequence of gel structure which caused different extents of pepsin diffusion into the gels. Later,
398 Somaratne et al. (2020b) partially confirmed this hypothesis by quantifying significant different
399 effective diffusion coefficients of FITC-pepsin in differently structured EWG, using the FRAP
400 technique. It is noteworthy that these different gel structures were obtained by heat gelation of EW
401 proteins previously adjusted to different pH (5 to 9). Therefore, Somaratne et al. (2020c)
402 underlined that the local pH in the micro-environment of the gastric enzyme might have also been
403 of paramount importance on the enzyme activity during the digestion process, and therefore on the
404 corresponding EW proteolysis kinetics. Using an identical *in vitro* digestion approach, the kinetics
405 of peptide release from the four different foods studied in the present work were determined (Hiolle
406 et al., 2020). Quite surprisingly, very comparable kinetics of proteolysis and peptide release were
407 observed despite the strong different structures generated by food processing. This result agreed
408 with Lorieau et al. (2018), who reported similar *in vitro* proteolysis rates for different heat-induced
409 whey protein gels, which had dissimilar structures but identical composition. To explain these
410 contradictory results, Hiolle et al. (2020) hypothesized that the diffusion of digestive proteases was

411 probably not significantly impacted by the structural properties of the different food matrices (from
412 liquid to hard solid). However, in the present study, we have demonstrated that the diffusion rates
413 of pepsin inside the foods are significantly impacted by their physical properties, with effective
414 diffusion coefficient varying exponentially according to their dry matter content (Figure 2). This
415 results clearly prove that the sole hypothesis mentioned in Hiolle et al. (2020) cannot be invoked
416 to explain the absence of structural effects on nutrients' release during gastric digestion. We can
417 however emphasize that *in vitro* digestion models are probably not sufficiently discriminating
418 methodology to highlight the structural effect of food on the mode of action of gastric enzymes.

419

420 **4. Conclusion**

421 This study is the first report on pepsin diffusion using the FRAP technique inside complex food
422 matrices of same composition on a dry matter basis but with different structures: one liquid food
423 (Custard), and three more or less dense and dry solid foods (Biscuit, Pudding, Sponge cake). The
424 results show that pepsin diffusivity within the solid particles is mainly conditioned by the dry
425 matter content of the product, following the stretched exponential equation with a very good fit.
426 This is likely because the dry matter content controls the density of the protein network and
427 therefore the amount of solvent phase, trapped in the structure and available for the diffusion of
428 hydrophilic compounds such as pepsin.

429 Thus, our results contribute to a better understanding of the digestion process and particularly the
430 gastric phase, using an engineering approach. Such knowledge could therefore assist to understand
431 the effect of complex food structure on digestion kinetics for desired nutritional and/or health
432 outcome. Moreover, the knowledge of the diffusion properties of pepsin in complex food particles
433 is of major importance as physical input parameter for mathematical reaction-diffusion models of

434 digestion that are currently developed in the food digestion research community (Le Feunteun et
435 al., 2021).

436 However, the present work investigated the diffusion behaviour of inactivated pepsin, due to the
437 labelling reaction with the fluorescent dye. In physiological conditions, pepsin diffusion through
438 the matrix might be accompanied by the disintegration of the food particles due to its enzymatic
439 activity, making the understanding of both phenomena even more difficult. Future research should
440 therefore focus on the effect of pepsin activity on its diffusion behaviour within protein based-food
441 particles during digestion.

442

443 **Credit author statement**

444 All authors contributed substantially to this work. E. Rakhshi, conducted the research and wrote
445 the manuscript, F. Nau acquired the funding and was the project administrator, provided expertise
446 regarding the chemical analysis, reviewed and edited the manuscript, M. Hiolle designed and
447 produced regarding the manufacturing process of the food matrices, and J. Floury designed the
448 experiments, provided expertise in terms of confocal microscopy, FRAP technique, image
449 analyses and data modelling, reviewed and edited the manuscript.

450

451 **Acknowledgment**

452 The authors thank Liot (Pleumartin, France) and Sotexpro (Bermericourt, France) for providing
453 raw ingredients (egg powders and pea flour respectively).

454 This work was supported by the French National Research Institute for Agriculture, Food and the
455 Environment (INRAE) and Carnot Qualiment. The ZEISS LSM880 confocal microscope was

456 funded by the European Union (FEDER), the French Ministry of Education, Research and
457 Innovation, the Regional Council of Brittany and INRAE.

458

459 The authors declare that there is no conflict of interest

460

461 **References**

462 **Agence Française de Normalisation (AFNOR). (1985). Fromages et fromages fondus -**
463 **Détermination de la matière sèche (méthode de référence). 4p.**

464 Amsden, B. (1998). Solute diffusion in hydrogels. Mechanisms and models. *Macromolecules*, *31*,
465 8382–8395.

466 Barbé, F., Ménard, O., Le Gouar, Y., Buffière, C., Famelart, M.-H., Laroche, B., Le Feunteun, S.,
467 Dupont, D., & Rémond, D. (2013). The heat treatment and the gelation are strong
468 determinants of the kinetics of milk proteins digestion and of the peripheral availability of
469 amino acids. *Food Chemistry*, *136*(3–4), 1203–1212.
470 <https://doi.org/10.1016/j.foodchem.2012.09.022>

471 Belton, P. S. (1999). Mini Review: On the Elasticity of Wheat Gluten. *Journal of Cereal Science*,
472 *29*(2), 103–107. <https://doi.org/10.1006/jcrs.1998.0227>

473 BeMiller, J. N. (2018). *Carbohydrate chemistry for food scientists* (3rd edition). Elsevier.

474 Braga, J., Desterro, J. M. P., & Carmo-Fonseca, M. (2004). Intracellular Macromolecular Mobility
475 Measured by Fluorescence Recovery after Photobleaching with Confocal Laser Scanning
476 Microscopes. *Molecular Biology of the Cell*, *15*(10), 4749–4760.
477 <https://doi.org/10.1091/mbc.e04-06-0496>

- 478 Capuano, E., & Janssen, A. E. M. (2021). Food Matrix and Macronutrient Digestion. *Annual*
479 *Review of Food Science and Technology*, 12, 193–212. [https://doi.org/10.1146/annurev-
480 food-032519-051646](https://doi.org/10.1146/annurev-
480 food-032519-051646)
- 481 Chapeau, A. L., Silva, J. V. C., Schuck, P., Thierry, A., & Floury, J. (2016). The influence of
482 cheese composition and microstructure on the diffusion of macromolecules: A study using
483 Fluorescence Recovery After Photobleaching (FRAP). *Food Chemistry*, 192, 660–667.
484 <https://doi.org/10.1016/j.foodchem.2015.07.053>
- 485 Chevallier, S., Colonna, P., Buléon, A., & Valle, G. D. (2000). Physicochemical Behaviors of
486 Sugars, Lipids, and Gluten in Short Dough and Biscuit. *Journal of Agricultural and Food*
487 *Chemistry*, 48(4), 1322–1326.
488 [https://www.academia.edu/17058208/Physicochemical_Behaviors_of_Sugars_Lipids_an
489 d_Gluten_in_Short_Dough_and_Biscuit](https://www.academia.edu/17058208/Physicochemical_Behaviors_of_Sugars_Lipids_an
489 d_Gluten_in_Short_Dough_and_Biscuit)
- 490 Cukier, R. I. (1984). Diffusion of Brownian spheres in semidilute polymer solutions.
491 *Macromolecules*, 17(2), 252–255. <https://doi.org/10.1021/ma00132a023>
- 492 de Kort, D. W., van Duynhoven, J. P. M., Van As, H., & Mariette, F. (2015). Nanoparticle
493 diffusometry for quantitative assessment of submicron structure in food biopolymer
494 networks. *Trends in Food Science & Technology*, 42(1), 13–26.
495 <https://doi.org/10.1016/j.tifs.2014.11.003>
- 496 Dekkers, B. L., Kolodziejczyk, E., Acquistapace, S., Engmann, J., & Wooster, T. J. (2016). Impact
497 of gastric pH profiles on the proteolytic digestion of mixed β lg-Xanthan biopolymer gels.
498 *Food & Function*, 7(1), 58–68. <https://doi.org/10.1039/c5fo01085c>

499 Fischer, T. (2004). Effect of extrusion cooking on protein modification in wheat flour. *European*
500 *Food Research and Technology*, 218(2), 128–132. [https://doi.org/10.1007/s00217-003-](https://doi.org/10.1007/s00217-003-0810-4)
501 0810-4

502 Hiolle, M., Lechevalier, V., Floury, J., Boulier-Monthéan, N., Prioul, C., Dupont, D., & Nau, F.
503 (2020). In vitro digestion of complex foods: How microstructure influences food
504 disintegration and micronutrient bioaccessibility. *Food Research International*, 128,
505 108817. <https://doi.org/10.1016/j.foodres.2019.108817>

506 Jin, Y., Yu, Y., Qi, Y., Wang, F., Yan, J., & Zou, H. (2016). Peptide profiling and the bioactivity
507 character of yogurt in the simulated gastrointestinal digestion. *Journal of Proteomics*, 141,
508 24–46. <https://doi.org/10.1016/j.jprot.2016.04.010>

509 Kamatari, Y. O., Dobson, C. M., & Konno, T. (2003). Structural dissection of alkaline-denatured
510 pepsin. *Protein Science : A Publication of the Protein Society*, 12(4), 717–724.

511 Kong, F., & Singh, R. P. (2010). A Human Gastric Simulator (HGS) to Study Food Digestion in
512 Human Stomach. *Journal of Food Science*, 75(9), E627–E635.
513 <https://doi.org/10.1111/j.1750-3841.2010.01856.x>

514 Grundy, M. M., Carrière, F., R. Mackie, A., A. Gray, D., J. Butterworth, P., & R. Ellis, P. (2016).
515 The role of plant cell wall encapsulation and porosity in regulating lipolysis during the
516 digestion of almond seeds. *Food & Function*, 7(1), 69–78.
517 <https://doi.org/10.1039/C5FO00758E>

518 Lorén, N., Hagman, J., Jonasson, J. K., Deschout, H., Bernin, D., Cella-Zanacchi, F., Diaspro, A.,
519 McNally, J. G., Ameloot, M., Smisdom, N., Nydén, M., Hermansson, A.-M., Rudemo, M.,
520 & Braeckmans, K. (2015). Fluorescence recovery after photobleaching in material and life

521 sciences: Putting theory into practice. *Quarterly Reviews of Biophysics*, 48(3), 323–387.
522 <https://doi.org/10.1017/S0033583515000013>

523 Lorén, N., Nydén, M., & Hermansson, A.-M. (2009). Determination of local diffusion properties
524 in heterogeneous biomaterials. *Advances in Colloid and Interface Science*, 150(1), 5–15.
525 <https://doi.org/10.1016/j.cis.2009.05.004>

526 Lorieau, L., Halabi, A., Ligneul, A., Hazart, E., Dupont, D., & Floury, J. (2018). Impact of the
527 dairy product structure and protein nature on the proteolysis and amino acid bioaccessibility
528 during in vitro digestion. *Food Hydrocolloids*, 82, 399–411.

529 Luo, Q., Borst, J. W., Westphal, A. H., Boom, R. M., & Janssen, A. E. M. (2017). Pepsin diffusivity
530 in whey protein gels and its effect on gastric digestion. *Food Hydrocolloids*, 66, 318–325.
531 <https://doi.org/10.1016/j.foodhyd.2016.11.046>

532 Luo, Q., Sewalt, E., Borst, J. W., Westphal, A. H., Boom, R. M., & Janssen, A. E. M. (2019).
533 Analysis and modeling of enhanced green fluorescent protein diffusivity in whey protein
534 gels. *Food Research International*, 120, 449–455.
535 <https://doi.org/10.1016/j.foodres.2018.10.087>

536 **Marze, S. (2013). Bioaccessibility of Nutrients and Micronutrients from Dispersed Food Systems:
537 Impact of the Multiscale Bulk and Interfacial Structures. *Critical Reviews in Food Science
538 and Nutrition*, 53(1), 76–108. <https://doi.org/10.1080/10408398.2010.525331>**

539 Masaro, L., & Zhu, X. X. (1999). Physical models of diffusion for polymer solutions, gels and
540 solids. *Progress in Polymer Science*, 24(5), 731–775. [https://doi.org/10.1016/S0079-
541 6700\(99\)00016-7](https://doi.org/10.1016/S0079-6700(99)00016-7)

542 Minekus, M., Alminger, M., Alvito, P., Ballance, S., Bohn, T., Bourlieu, C., Carrière, F., Boutrou,
543 R., Corredig, M., Dupont, D., Dufour, C., Egger, L., Golding, M., Karakaya, S., Kirkhus,

544 B., Feunteun, S. L., Lesmes, U., Macierzanka, A., Mackie, A., ... Brodkorb, A. (2014). A
545 standardised static in vitro digestion method suitable for food – an international consensus.
546 *Food & Function*, 5(6), 1113–1124. <https://doi.org/10.1039/C3FO60702J>

547 Morell, P., Fiszman, S., Llorca, E., & Hernando, I. (2017). Designing added-protein yogurts:
548 Relationship between in vitro digestion behavior and structure. *Food Hydrocolloids*, 72,
549 27–34. <https://doi.org/10.1016/j.foodhyd.2017.05.026>

550 Nicolai, T., Durand, D., & Durand, D. (2012). Relation between the gel structure and the mobility
551 of tracers in globular protein gels. *Journal of Colloid and Interface Science*, 388(1), 293–
552 299. <https://doi.org/10.1016/j.jcis.2012.08.032>

553 Norton, J. E., Wallis, G. A., Spyropoulos, F., Lillford, P. J., & Norton, I. T. (2014). Designing food
554 structures for nutrition and health benefits. *Annual Review of Food Science and*
555 *Technology*, 5, 177–195. <https://doi.org/10.1146/annurev-food-030713-092315>

556 Nyemb, K., Guérin-Dubiard, C., Pézennec, S., Jardin, J., Briard-Bion, V., Cauty, C., Rutherford,
557 S. M., Dupont, D., & Nau, F. (2016). The structural properties of egg white gels impact the
558 extent of in vitro protein digestion and the nature of peptides generated. *Food*
559 *Hydrocolloids*, 54, Part B, 315–327. <https://doi.org/10.1016/j.foodhyd.2015.10.011>

560 Phillies, G. D. J. (1986). Universal scaling equation for self-diffusion by macromolecules in
561 solution. *Macromolecules*, 19(9), 2367–2376. <https://doi.org/10.1021/ma00163a006>

562 Phillies, G. D. J. (2016). The Hydrodynamic Scaling Model for the Dynamics of Non-Dilute
563 Polymer Solutions: A Comprehensive Review. *ArXiv:1606.09302 [Cond-Mat]*.
564 <http://arxiv.org/abs/1606.09302>

565 Rinaldi, L., Gauthier, S. F., Britten, M., & Turgeon, S. L. (2014). In vitro gastrointestinal digestion
566 of liquid and semi-liquid dairy matrixes. *LWT - Food Science and Technology*, 57(1), 99–
567 105. <https://doi.org/10.1016/j.lwt.2014.01.026>

568 Shewry, P. R., & Tatham, A. S. (1997). Disulphide Bonds in Wheat Gluten Proteins. *Journal of*
569 *Cereal Science*, 25(3), 207–227. <https://doi.org/10.1006/jcrs.1996.0100>

570 Silva, J. V. C., Peixoto, P. D. S., Lortal, S., & Flourey, J. (2013). Transport phenomena in a model
571 cheese: The influence of the charge and shape of solutes on diffusion. *Journal of Dairy*
572 *Science*, 96(10), 6186–6198. <https://doi.org/10.3168/jds.2013-6552>

573 Somaratne, G., Ferrua, M. J., Ye, A., Nau, F., Flourey, J., Dupont, D., & Singh, J. (2020). Food
574 material properties as determining factors in nutrient release during human gastric
575 digestion: A review. *Critical Reviews in Food Science and Nutrition*, 1–17.
576 <https://doi.org/10.1080/10408398.2019.1707770>

577 Somaratne, G., Nau, F., Ferrua, M. J., Singh, J., Ye, A., Dupont, D., Singh, R. P., & Flourey, J.
578 (2020a). Characterization of egg white gel microstructure and its relationship with pepsin
579 diffusivity. *Food Hydrocolloids*, 98. Scopus.
580 <https://doi.org/10.1016/j.foodhyd.2019.105258>

581 Somaratne, G., Nau, F., Ferrua, M. J., Singh, J., Ye, A., Dupont, D., Singh, R. P., & Flourey, J.
582 (2020b). In-situ disintegration of egg white gels by pepsin and kinetics of nutrient release
583 followed by time-lapse confocal microscopy. *Food Hydrocolloids*, 98, 105228.
584 <https://doi.org/10.1016/j.foodhyd.2019.105228>

585 Thévenot, J., Cauty, C., Legland, D., Dupont, D., & Flourey, J. (2017). Pepsin diffusion in dairy
586 gels depends on casein concentration and microstructure. *Food Chemistry*, 223, 54–61.
587 <https://doi.org/10.1016/j.foodchem.2016.12.014>

588 Woodward, S. A., & Cotterill, O. J. (1987). Texture Profile Analysis, Expressed Serum, and
589 Microstructure of Heat-Formed Egg Yolk Gels. *Journal of Food Science*, 52(1), 68–74.
590 <https://doi.org/10.1111/j.1365-2621.1987.tb13974.x>

591 Yamashita, H., Ishibashi, J., Hong, Y.-H., & Hirose, M. (1998). Involvement of Ovotransferrin in
592 the Thermally Induced Gelation of Egg White at around 65.DEG.C.. *Bioscience,*
593 *Biotechnology, and Biochemistry*, 62(3), 593–595. <https://doi.org/10.1271/bbb.62.593>

594

Table 1.





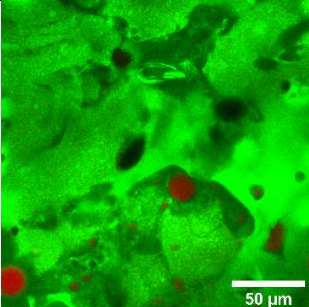
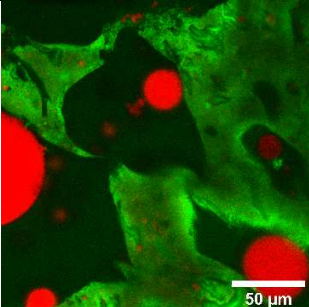
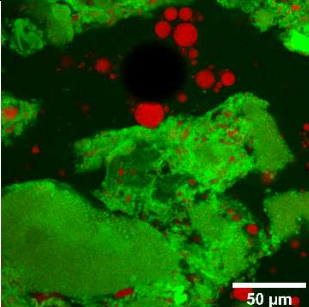
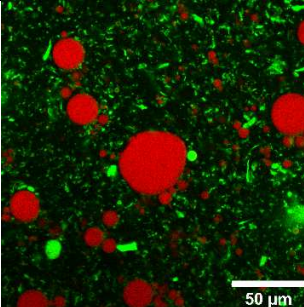
| Food matrix | Biscuit | Sponge cake | Pudding | Custard |
|---|--|---|--|--|
| Main process steps | Kneading-Cooking | Whisking-Mixing-Cooking | Mixing-Cooking | Mixing-Cooking |
| Cooking temperature and duration | 180°C - 18 min | 180°C - 30 min | 180°C - 20 min | 110°C - 20 min |
| Water content after cooking (g/100g) <i>Mean value ± SD</i> | 5.56 ± 1.59 | 38.29 ± 3.48 | 48.26 ± 1.70 | 68.44 ± 0.05 |
| Macroscopic aspect <i>(Photography)</i> |  |  |  |  |
| Microstructure <i>(CSLM observations, magnification x40, fat appears in red, proteins in green)</i> |  |  |  |  |

Table 2.

| Sample (Dry Matter %) | Effective diffusion coefficient D_{eff} ($\mu\text{m}^2/\text{s}$) | Reduced diffusion coefficient D_r |
|------------------------------|--|---|
| <i>Water (0%)</i> | 138 ± 11^a | 1.00 ± 0.08 |
| Custard (31.6%) | 48 ± 14^b | 0.35 ± 0.10 |
| Pudding (51.7%) | 19 ± 11^c | 0.14 ± 0.08 |
| Sponge cake (61.7%) | 17 ± 8^c | 0.13 ± 0.05 |
| Biscuit (94.4%) | 2 ± 1^d | 0.013 ± 0.006 |

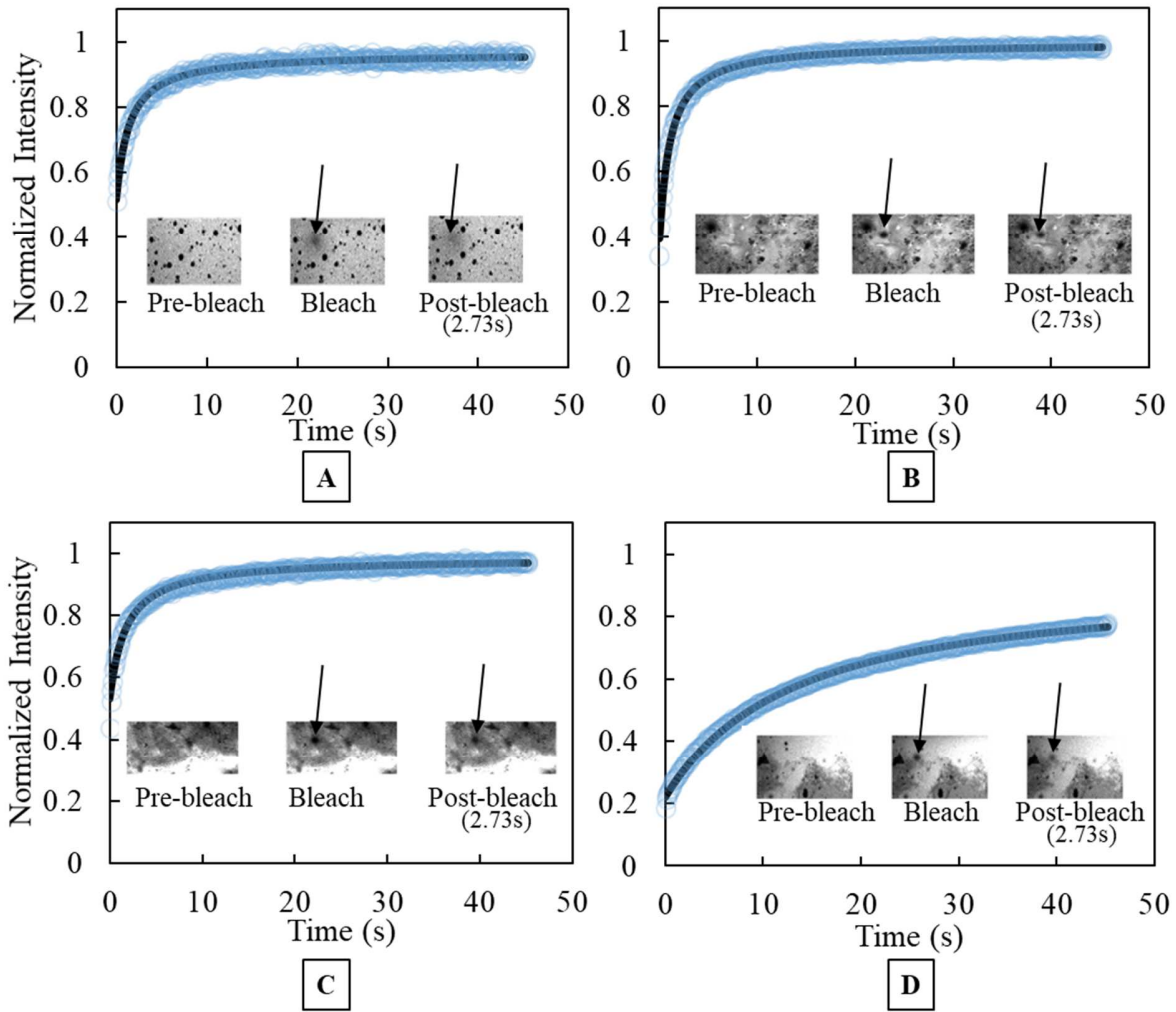


Figure 1.

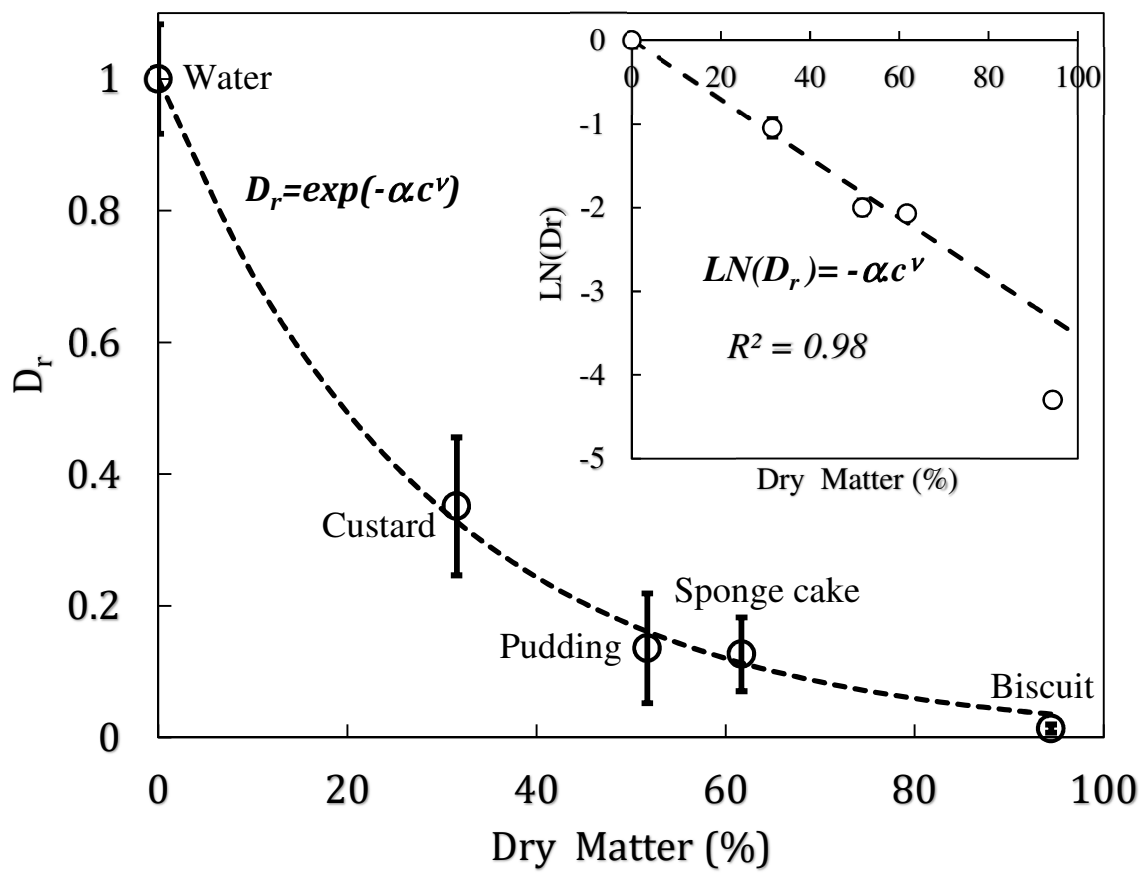


Figure 2.

Table captions

Table 1. Overview of the designed matrices.

Table 2. Effective diffusion coefficient (D_{eff}) and reduced diffusion coefficient (D_r) of FITC-pepsin in the four food matrices and in water at 37°C. Values are means \pm SD (n=30). Different letters represent statistically significant differences ($p < 0.05$).

Figure captions

Figure 1. Representative FRAP profiles and images before bleaching and after 0 and 2.73 s for diffusion of FITC-pepsin in Custard (a), Pudding (b), Sponge cake (c), and Biscuit (d). Solid lines (in black) denote the best data curve fit to the experimental data (in blue). Arrows indicate the area where the Region of Interest (ROI) was localized for bleaching experiments.

Figure 2. Reduced diffusion coefficient of FITC-pepsin in food matrices with different dry matter content (DM). The dotted line represents the “universal” stretched exponential equation applied to the experimental data (circle).